Crone control of a nonlinear hydraulic actuator

Valérie Pommier[a,*], Jocelyn Sabatier[b], Patrick Lanusse[b], Alain Oustaloup[b]

[a] *ENSERB, LAP Equipe CRONE Team, Université Bordeaux I, 351 Cours de la Libération, 33405 Talence Cedex, France*
[b] *LAMEFIP-ENSAM, 351 Cours de la Libération, 33405 Talence Cedex, France*

Received 21 June 2000; accepted 28 September 2001

Abstract

The CRONE control (fractional robust control) of a hydraulic actuator whose dynamic model is nonlinear is presented. An input–output linearization under diffeomorphism and feedback is first achieved for the nominal plant. The relevance of this linearization when the parameters of the plant vary is then analyzed using the Volterra input–output representation in the frequency domain. CRONE control based on complex fractional differentiation is finally applied to control the velocity of the input–output linearized model when parametric variations occur. © 2002 Elsevier Science Ltd. All rights reserved.

Keywords: CRONE (fractional robust) control; Nonlinear system; Linearization; Volterra series; Hydraulic actuator

1. Introduction

To design a linear control system for a nonlinear plant, a linear model can be extracted from the nonlinear model using the first order linearization. To avoid this approximation, input–output linearization under diffeomorphism and feedback (Levine, 1996) is often used and transforms a nonlinear plant into a linear plant. Several studies have applied this method to hydraulic actuators and demonstrated that better dynamic performance is achieved with an input–output linearized model than with a first order linear model. However, the robustness of the control system when parametric variations or perturbations occur has been mentioned but not investigated (Brun, Belghardi, Sesmat, Thomasset, & Scavarda, 1999).

As the linearizing system is computed only for the nominal parametric state, the plant behavior remains nonlinear for the other parametric states. The question is then whether this partially input–output linearized plant is less sensitive to parametric variations than the initial nonlinear plant. To evaluate this sensitivity to parametric variations, the Volterra representation (Brockett, 1976; Lesiar & Krener, 1978) can be used. Indeed, an input–output representation of the input–output linearized plant can be given by a Volterra series. The first term of the series is the first order linear model, and the magnitude of the other terms depend on the nonlinearity: the stronger the nonlinearity, the higher the modulus of each term.

Once the input–output linearization is achieved, a set of first order linear models can be computed from the perturbed input–output "linearized" plant. CRONE control, which is a robust linear control-system design based on complex-order differentiation, can then be applied to the set. Considering the robustness/performance-quality trade-off, the plant perturbations can be taken into account by using fully structured frequency uncertainty domains to obtain a least-conservative control system.

The article is organized as following. Section 2 gives a description and a model of the hydraulic system under study. Section 3 deals with the input–output linearization under diffeomorphism and static feedback, and shows the importance of the choice of the linearizing system in the case of robust control. In Section 4, the input–output representation using a Volterra series, particularly in the frequency domain, is developed. The Volterra representation is then used to compare the perturbed input–output "linearized" plant to the initial nonlinear plant. Finally in Section 5, CRONE control (Oustaloup & Mathieu, 1999) is introduced and applied to the electrohydraulic system.

2. Electrohydraulic system

2.1. Electrohydraulic system description

The electrohydraulic system under study is part of a test bench for mechanical structures (Fig. 1). These structures must be deformed by the electrohydraulic actuator at constant velocity (Fig. 2). The actuator is a double-acting 200 mm stroke cylinder. A servovalve fed with a fixed displacement hydraulic pump supplies a constant pressure. The piston rod is connected to a mechanical structure modeled by a mass-damper-spring set. The values of the structure parameters vary during the test since the structure is deformed. The variations are assumed to be slow compared to the control loop dynamic. The cylinder chambers are each fitted with a pressure sensor. Position, velocity and acceleration are provided by sensors on the piston rod.

2.2. Plant modeling

The complete plant model is obtained from the models of the electrohydraulic servovalve, of the cylinder and of the mechanical part (Cloy & Martin, 1980; Merrit, 1967).

The electrohydraulic servovalve is composed of several stages whose main ones are the amplification stage and the flow stage. In the amplification stage, a spool is actuated by an electromechanical system with the input current u as control effort. This stage is modeled by a two-order state-space model where y_u is the spool position and where v_u is $\dot{y}_u$:

$$\begin{bmatrix} \dot{v}_u \\ \dot{y}_u \end{bmatrix} = \begin{bmatrix} -2\zeta_n\omega_n & -\omega_n^2 \\ 1 & 0 \end{bmatrix} \begin{bmatrix} v_u \\ y_u \end{bmatrix} + \begin{bmatrix} k\omega_n^2 \\ 0 \end{bmatrix} u. \tag{1}$$

In the flow stage, the spool slides in a sleeve which controls the flows provided to the cylinder chambers. To model these flows, the Bernoulli equation is applied between two points of the sleeve.

The mass flow rate Q is thus proportional to $S\sqrt{\Delta P}$, where S is the effective area of the restrictions of the sleeve and ΔP the pressure-difference between the two points. Given that S is proportional to y_u and that leaks can be neglected, the flow mass rates to each cylinder chamber, Q_1 and Q_2, are described by

$$Q_1(y_u, P_1) = \begin{cases} y_u\sqrt{|P_s - P_1|}\,\mathrm{sign}(P_s - P_1) & \text{for } y_u \geqslant 0 \\ y_u\sqrt{|P_1 - P_r|}\,\mathrm{sign}(P_1 - P_r) & \text{for } y_u < 0 \end{cases}$$

$$Q_2(y_u, P_2) = \begin{cases} -y_u\sqrt{|P_2 - P_r|}\,\mathrm{sign}(P_2 - P_r) & \text{for } y_u \geqslant 0 \\ -y_u\sqrt{|P_s - P_2|}\,\mathrm{sign}(P_s - P_2) & \text{for } y_u < 0. \end{cases} \tag{2}$$

Here, the proportional gain (between Q and $S\sqrt{\Delta P}$) does not appear because it is already taken into account in parameter k of the amplification stage (1). As the flow

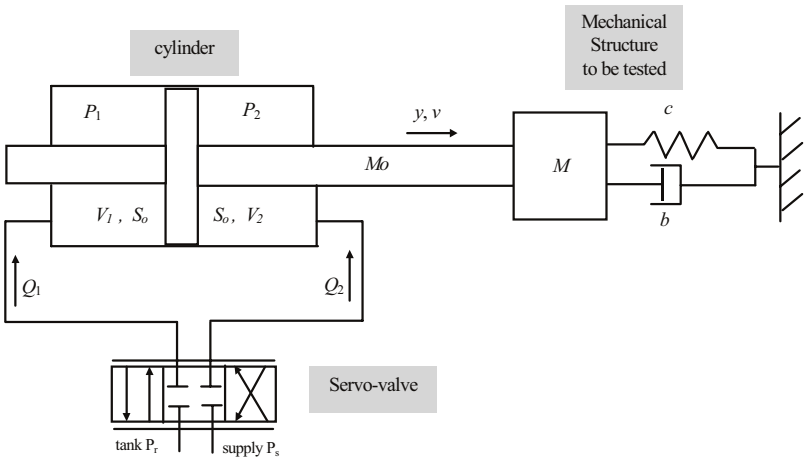

Fig. 1. Electrohydraulic system and test structure.

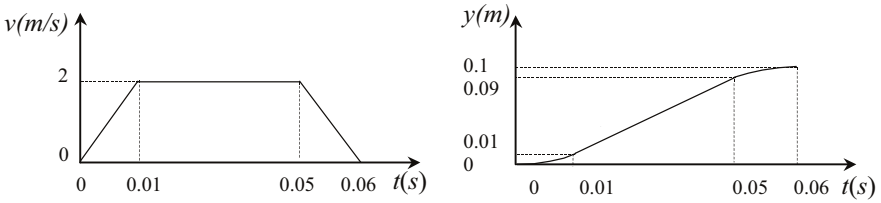

Fig. 2. Piston rod velocity and trajectory.

stage is symmetric, $Q_1(y_u, P_1) = -Q_2(y_u, P_2)$, which implies $P_s + P_r = P_1 + P_2 \ \forall y_u$.

The cylinder is modeled using the thermodynamic equation giving the pressure behavior:

$$\frac{V}{B}\frac{\mathrm{d}P}{\mathrm{d}t} + \frac{\mathrm{d}V}{\mathrm{d}t} = Q,$$

where B is the bulk isotherm modulus, and where V, P and Q are respectively: volume, pressure and mass flow rate in a cylinder chamber. For the electrohydraulic system under study, the mass flow rates Q_1 and Q_2 are given by (2). Volumes are: $V_1 = V_0 + S_0 y$ and $V_2 = V_0 - S_0 y$, where S_0 is the cylinder rod effective area and V_0 the half-volume. Thus the pressure behaviors in the two cylinder chambers are described by

$$\frac{\mathrm{d}P_1}{\mathrm{d}t} = \frac{B}{V_0 + S_0 y}(Q_1 - S_0 v)$$

and

$$\frac{\mathrm{d}P_2}{\mathrm{d}t} = \frac{B}{V_0 - S_0 y}(Q_2 + S_0 v). \tag{3}$$

Concerning the mechanical part, the model is obtained from the fundamental dynamic equation:

$$(M + M_0)\frac{\mathrm{d}^2 y}{\mathrm{d}t^2} = S_0 P_1 - S_0 P_2 - bv - cy - F_f, \tag{4}$$

where F_f represents the Coulomb, Static and Stribeck friction force (Olsson, Aström, Canudas de Wit, Gäfvert, & Lischinsky, 1998) and expresses:

$$F_f = F_c \mathrm{sgn}(v) + (F_s - F_c)\mathrm{e}^{(-v/v_s)^2}\mathrm{sgn}(v). \tag{5}$$

Finally, as the controlled output is the velocity, the state space model of the electrohydraulic system obtained from Eqs. (2)–(4) is:

$$\begin{cases} \dot{\mathbf{X}} = \mathbf{f_1}(\mathbf{X}) + \mathbf{g}(\mathbf{X})u & \text{for } y_u \geqslant 0 \\ \dot{\mathbf{X}} = \mathbf{f_2}(\mathbf{X}) + \mathbf{g}(\mathbf{X})u & \text{for } y_u < 0 \ \text{ with } \mathbf{X} = (v_u \ \ y_u \ \ P_1 \ \ P_2 \ \ v \ \ y)^{\mathrm{T}}. \\ \mathbf{Y} = \mathbf{h}(\mathbf{X}) \end{cases} \tag{6}$$

This is a six-order nonlinear model where $\mathbf{f}_1$, $\mathbf{f}_2$, $\mathbf{g}$ and $\mathbf{h}$ are defined by

$$\mathbf{f}_1(\mathbf{X}) = \begin{pmatrix} -2\zeta_n\omega_n v_u - \omega_n^2 y_u \\ v_u \\ -\dfrac{B}{V_0 + S_0 y}S_0 v + \dfrac{B}{V_0 + S_0 y}\sqrt{|P_s - P_1|}\mathrm{sign}(P_s - P_1)y_u \\ \dfrac{B}{V_0 - S_0 y}S_0 v - \dfrac{B}{V_0 - S_0 y}\sqrt{|P_2 - P_r|}\mathrm{sign}(P_2 - P_r)y_u \\ \dfrac{1}{M + M_0}(S_0 P_1 - S_0 P_2 - cy - bv - F_f) \\ v \end{pmatrix}, \tag{7}$$

$$\mathbf{f}_2(X) = \begin{pmatrix} -2\zeta_n\omega_n v_u - \omega_n^2 y_u \\ v_u \\ -\dfrac{B}{V_0 + S_0 y}S_0 v + \dfrac{B}{V_0 + S_0 y}\sqrt{|P_1 - P_r|}\mathrm{sign}(P_1 - P_r)y_u \\ \dfrac{B}{V_0 - S_0 y}S_0 v - \dfrac{B}{V_0 - S_0 y}\sqrt{|P_s - P_2|}\mathrm{sign}(P_s - P_2)y_u \\ \dfrac{1}{M + M_0}(S_0 P_1 - S_0 P_2 - cy - bv - F_f) \\ v \end{pmatrix}, \tag{8}$$

$$\mathbf{g}(\mathbf{X}) = (k\omega_n^2 \quad 0 \quad 0 \quad 0 \quad 0 \quad 0)^{\mathrm{T}} \text{ and } \mathbf{h}(\mathbf{X}) = v. \tag{9}$$

3. Input–output linearization under diffeomorphism and static feedback of the electrohydraulic system

3.1. Results concerning the input–output linearization of a square nonlinear system

Let (Σ) be a square nonlinear system of dimension m:

$$\begin{cases} \dot{\mathbf{X}} = \mathbf{f}(\mathbf{X}) + \sum_{i\in m}\mathbf{g}_i(\mathbf{X})\mathbf{u}_i \\ \mathbf{Y} = \mathbf{h}(\mathbf{X}) \end{cases}, \mathbf{u}\in\mathbb{R}^m, \mathbf{Y}\in\mathbb{R}^m, \mathbf{X}\in\mathbb{R}^n, \tag{10}$$

assuming that:

- the vectors fields $\mathbf{f}(\mathbf{X})$ and $\mathbf{g}_i(\mathbf{X})$ are analytic functions,
- $\mathbf{h}(\mathbf{X})$ is an analytic submersion. Locally, $\mathbf{h}$ is given by $[\mathbf{h}_1(\mathbf{X}), ..., \mathbf{h}_m(\mathbf{X})]$ with $\mathbf{h}_i(\mathbf{X})$ from $\mathbb{R}^m$ to $\mathbb{R}$,
- $\mathbf{Y} = [\mathbf{Y}_1(\mathbf{X}), \ldots, \mathbf{Y}_i(\mathbf{X}), \ldots, \mathbf{Y}_m(\mathbf{X})]$.

Let $(\rho_1, \ldots, \rho_m)$ be the set of row infinite vectors of the system (Σ) defined as follows:

$$\rho_i = \{\inf(l)\in\mathbb{N}/\exists j\in m, L_{\mathbf{g}_j}L_{\mathbf{f}}^{l-1}\mathbf{h}_i \neq 0\}, \tag{11}$$

where $L_{\mathbf{f}}$ being the Lie derivative (Isidori, 1995) (Slotine & Li, 1991) (Krstic, Kanellakopoulos, & Kokotovic, 1995) with respect to the vector field $\mathbf{f}$ given by

$$L_{\mathbf{f}}(\mathbf{X}) = \sum_{i=1}^{n}\mathbf{f}_i(\mathbf{X})\frac{\partial}{\partial \mathbf{X}_i}.$$

ρ_i corresponds to the first $\mathbf{Y}_i$ derivative which makes $\mathbf{u}$ appear explicitly and verifies:

$$\mathbf{Y}^{(\rho_i)} = L_{\mathbf{f}}^{\rho_i}(\mathbf{X}) + L_{\mathbf{g}}L_{\mathbf{f}}^{\rho_i - 1}\mathbf{h}(\mathbf{X})\mathbf{u}. \tag{12}$$

Let $\mathbf{\Delta}(\mathbf{X})$ be the decoupling matrix of the system and $\mathbf{\Delta}_0(\mathbf{X})$ the compensation vector respectively defined by

$$\mathbf{\Delta}(\mathbf{X}) = \begin{bmatrix} L_{\mathbf{g}_1}L_{\mathbf{f}}^{\rho_1 - 1}\mathbf{h}_1(\mathbf{X}) & \ldots & L_{\mathbf{g}_m}L_{\mathbf{f}}^{\rho_1 - 1}\mathbf{h}_1(\mathbf{X}) \\ \ldots & \ldots & \ldots \\ L_{\mathbf{g}_1}L_{\mathbf{f}}^{\rho_m - 1}\mathbf{h}_m(\mathbf{X}) & \ldots & L_{\mathbf{g}_m}L_{\mathbf{f}}^{\rho_m - 1}\mathbf{h}_m(\mathbf{X}) \end{bmatrix} \tag{13}$$

and

$$\mathbf{\Delta}_0(X) = \begin{bmatrix} L_{\mathbf{f}}^{\rho_1}\mathbf{h}_1(\mathbf{X}) \\ \dots \\ L_{\mathbf{f}}^{\rho_m}\mathbf{h}_m(\mathbf{X}) \end{bmatrix}. \tag{14}$$

Theorem (Fossard & Normand-Cyrot, 1995). (i) *The system* (Σ) *can be decoupled statically on a submanifold* M_0 *of* $\mathbb{R}^m$ *if and only if rank* $\mathbf{\Delta}(\mathbf{X}) = m$, $\forall \mathbf{X} \in M_0$.

(ii) *If this condition for* $\mathbf{\Delta}(\mathbf{X})$ *is fulfilled, the state feedback defined by*

$$\mathbf{u}(\mathbf{X}) = \alpha(\mathbf{X}) + \beta(\mathbf{X})\mathbf{e} \tag{15}$$

with

$$\alpha(\mathbf{X}) = -\mathbf{\Delta}(\mathbf{X})^{-1}\mathbf{\Delta}_0(\mathbf{X}) \text{ and } \beta(\mathbf{X}) = \mathbf{\Delta}(\mathbf{X})^{-1}, \tag{16}$$

decouples the system (Σ) *on* M_o.

(iii) *Simple calculation from relation* (12) *shows that the linearized system is a cascade of* ρ_i *integrators such as*

$$Y_i^{(\rho_i)} = e_i, \forall i \in m,$$

e_i *being a linearized system input. The system is said to have relative degree vector* $\rho = [\rho_1 \dots \rho_m]^{\mathrm{T}}$.

3.2. Choice of the linearizing system for robust control

To ensure stability robustness and to give a better dynamic behavior to the linearized plant, the following linearizing system is adopted:

$$\begin{pmatrix} u_1(\mathbf{X}) \\ \vdots \\ u_m(\mathbf{X}) \end{pmatrix} = \mathbf{\Delta}^{-1}(\mathbf{X}) \left[\begin{pmatrix} k_{u_1} e_1 \\ \vdots \\ k_{u_m} e_m \end{pmatrix} - \begin{pmatrix} \sum_{j=0}^{\rho_1 - 1} \alpha_{1j} Y_1^{(j)} \\ \vdots \\ \sum_{j=0}^{\rho_i - 1} \alpha_{mj} Y_m^{(j)} \end{pmatrix} - \mathbf{\Delta}_0(\mathbf{X}) \right] \tag{17}$$

which leads to the linearized plant:

$$H_i(s) = \frac{Y_i(s)}{E_i(s)} = \frac{k_{ui}}{s^{\rho_i} + \sum_{j=0}^{\rho_i - 1} \alpha_{ij} s^j}. \tag{18}$$

By adding the terms $\sum_{j=0}^{\rho_i - 1} \alpha_{ij} Y_i^{(j)}$, the linearizing feedback contains a part of the tracking feedback.

The choice of coefficients α_{ij} is important for stability robustness. Indeed, when parametric variations occur, the poles of the transfer function $H_i(s)$, $i \in [1, m]$, may move to the right half-plane if coefficients α_{ij} are badly chosen. Thus, coefficients α_{ij} must be chosen so that the poles of $H_i(s)$ are not too close to the imaginary axis.

Moreover, k_{ui} and α_{ij} must be chosen to respect the natural behavior of the plant so that it is not too solicited by the linearizing system. Consequently k_{ui} and α_{ij} are computed so that the frequency response of $H_i(s)$ is comparable to the first order linear model of a nominal nonlinear plant.

3.3. Input–output linearization of the electrohydraulic system

For the system under study, $\mathbf{f}(\mathbf{X})$ is not everywhere smooth because of the discontinuity in the model at $y_u = 0$. In order to take the Lie derivative, the vector field $\mathbf{f}$ is required to be smooth. We assume that the piston rod trajectory under study is such that $y_u \geqslant 0$. Thus the linearization is only achieved for positive y_u and hence $\mathbf{f}$ is smooth.

For the SISO electrohydraulic system under study, computations lead to a relative degree $\rho = 4$ and to:

- the decoupling term: $\mathbf{\Delta}(\mathbf{X}) = L_{\mathbf{g}} L_{\mathbf{fl}}^3 \mathbf{h}(\mathbf{X})$;
- the compensation term: $\mathbf{\Delta}_0(\mathbf{X}) = L_{\mathbf{fl}}^4 \mathbf{h}(\mathbf{X})$.

So, according to relation (17) and velocity v being the considered output, the linearizing system is:

$$u(\mathbf{X}) = \frac{1}{\mathbf{\Delta}(\mathbf{X})} \left[k_u e - \sum_{j=0}^{3} \alpha_j v^{(j)} - \mathbf{\Delta}_0(\mathbf{X}) \right], \tag{19}$$

which leads to the linearized system:

$$H(s) = \frac{k_u}{s^4 + \alpha_3 s^3 + \alpha_2 s^2 + \alpha_1 s + \alpha_0}.$$

As explained above, coefficients k_u and α_j are computed from the first order linear model of the nonlinear model given by (6) using the nominal values of Table 1. But, as the first order linear model has a very low damping coefficient ($\zeta = 0.02$), a higher damping coefficient is chosen ($\zeta = 0.2$) for $H(s)$ to prevent the poles of the perturbed "linearized" plant from moving to the right half-plane.

Table 1
Nomenclature

Variable names	Variable definitions	Values
P_s	Supply pressure	280 bar
P_r	Tank pressure	1 bar
P_1, P_2	Cylinder chamber pressures	Bar
Q_1, Q_2	Mass flow to the cylinder chambers from the servovalve	m^3/s
V_1, V_2	Cylinder chamber volumes	m^3
V_0	Cylinder half-volume	$5 \times 10^{-4}\,m^3$
M_0	Cylinder rod mass	50 kg
S_0	Cylinder rod effective area	$1.53 \times 10^{-3}\,m^2$
M	Test structure mass	$20\,kg \pm 50\%$
c	Test structure spring	$100000\,N/m \pm 50\%$
b	Test structure viscous coefficient	$200\,N/m\,s \pm 50\%$
y	Cylinder rod position	M
v	Cylinder rod velocity	m/s
k	Servovalve gain	$5.1 \times 10^{-5}\,m/V$
ω_n	Servovalve corner frequency	500 rad/s
ζ_n	Servovalve damping factor	0.4

Finally $k_u = 9.29475 \times 10^{12}, \alpha_0 = 7.25 \times 10^{10}, \alpha_1 = 1.7 \times 10^8, \alpha_2 = 6.28 \times 10^5$ and $\alpha_3 = 3$.

3.4. Behavior of the perturbed input–output linearized plant

Since the linearizing system is computed only for the nominal parametric state of the plant, the input–output linearized plant remains nonlinear for other parametric states. Indeed if $\mathbf{\Delta}_{\text{nom}}(\mathbf{X})$ and $\mathbf{\Delta}_{0\text{nom}}(\mathbf{X})$ are the decoupling and compensation terms calculated for the nominal plant, the output (velocity v) of the perturbed input–output linearized plant is given by

$$v^{(4)} = \mathbf{\Delta}_0(\mathbf{X}) + \mathbf{\Delta}(\mathbf{X}) \frac{1}{\mathbf{\Delta}_{\text{nom}}(\mathbf{X})} \times \left[k_u e - \sum_{j=0}^{3} \alpha_j v^{(j)} - \mathbf{\Delta}_{0\text{nom}}(\mathbf{X}) \right]. \quad (20)$$

As this model is nonlinear, to obtain a linear model for computing controller $C(s)$ of Fig. 8, a set of first order linear models is computed around the reference trajectory described in Fig. 2. This set must also be computed considering the parameter variations of the tested mechanical structure which are non-negligible since the structure is deformed during the test. The parameter variations are estimated at $\pm 50\%$ of the nominal values (given in Table 1) and may occur simultaneously.

4. Analysis of the input–output linearized electrohydraulic system using Volterra representation

4.1. Definition

Let (Σ) be the nonlinear system:

$$\begin{cases} \dot{\mathbf{X}} = \mathbf{f}(t, \mathbf{X}(t)) + \mathbf{g}(t, \mathbf{X}(t))u(t) \\ Y = h(t, \mathbf{X}(t)) \end{cases} \quad (21)$$

with $\mathbf{X} \in \mathbb{R}^n$, $u \in \mathbb{R}^n$, $\mathbf{X}(0) = \mathbf{X}_0$, $\mathbf{f}$ analytic functions on $\mathbb{R}^n$, $\mathbf{g}$ analytic function on $\mathbb{R}^n$, $\mathbf{f}(\mathbf{X}) = [f^1(\mathbf{X}), \ldots, f^n(\mathbf{X})]$, and $\mathbf{g}(\mathbf{X}) = [g^1(\mathbf{X}), \ldots, g^n(\mathbf{X})]$.

Definition (Lamnabhi-Lagarrigue, 1994). System (Σ) admits a Volterra series representation, if there are locally bounded and piecewise continuous functions:

$w_n : R^{n+1} \to R, n \in \mathbb{N}^*$,

with the following condition:

$\forall T > 0$, $\exists \varepsilon(T) > 0$ such that for any piecewise continuous function $u(.)$ verifying $|u(T)| \leqslant \varepsilon$ on $[0, T]$,

$$Y(t) = w_0(t) + \sum_{n=1}^{\infty} \int_{t0}^{t} \ldots \int_{t0}^{t} w_n(t, \sigma_1, \ldots, \sigma_n) \times u(\sigma_1) \ldots u(\sigma_n) \mathrm{d}\sigma_1 \ldots \mathrm{d}\sigma_n \quad (22)$$

converge absolutely and uniformly on $[0, T]$.

Function $w_n(t, \sigma_1, ..., \sigma_n)$ is called the degree-n Volterra kernel.

Remark. A kernel which verifies the relation $w_n(t, \sigma_1, \ldots, \sigma_n) = w_n(t, \sigma_{\Pi(1)}, \ldots, \sigma_{\Pi(n)})$, where Π is a permutation of σ_i, $w_n(t, \sigma_1, ..., \sigma_n)$, is said symmetric.

Hypothesis. For the next developments, the nonlinear system to be represented by a Volterra series is supposed to verify the following conditions:

1. initial conditions are null (which can always be obtained by a variable change);
2. the system is causal;
3. the system is stationary.

Also:

1. implies that function $w_0(t)$ is null;
2. implies that each degree-n kernel is realizable: $w_n(t, \sigma_1, ..., \sigma_n) = 0 \; \forall \sigma_i > t, i \in [1, n]$;
3. implies that each degree-n kernel can be written:

$$w_n(t, \sigma_1, ..., \sigma_n) = h_n(t - \sigma_i, ..., t - \sigma_n) = h_n(\tau_1, ..., \tau_n).$$

Relation (22) then becomes:

$$Y(t) = \sum_{n=0}^{\infty} \int_{-\infty}^{+\infty} \ldots \int_{-\infty}^{+\infty} h_n(\tau_1, \ldots, \tau_n) \prod_{i=1}^{n} u(t - \tau_i) \mathrm{d}\tau_i. \quad (23)$$

4.2. Computation of Volterra kernels in the frequency domain

The Fourier transform for a mono-variable function can be extended to a n-variable function $h_n(t_1, ..., t_n)$ (Billings & Jones, 1990):

$$H_n(\mathrm{j}\omega_1, \ldots, \mathrm{j}\omega_n) = \int_0^{\infty} \ldots \int_0^{\infty} h_n(\tau_1, \ldots, \tau_n) \times \mathrm{e}^{-\mathrm{j}\omega_1\tau_1 - \ldots - \mathrm{j}\omega_n\tau_n} \mathrm{d}\tau_1 \ldots \mathrm{d}\tau_n. \quad (24)$$

In the case of a Volterra representation, let $H_n(\mathrm{j}\omega_1, \ldots, \mathrm{j}\omega_n)$ be the Fourier transform of a degree-n kernel $h_n(\tau_1, ..., \tau_n)$.

The Fourier transform can be computed using the growing exponential approach introduced by (Rugh, 1981).

To describe this approach, take a degree-N system defined by

$$Y(t) = \int_{-\infty}^{+\infty} \int_{-\infty}^{+\infty} h_N(\tau_1, \ldots, \tau_n) u(t - \tau_1) \ldots u(t - \tau_N) \mathrm{d}\tau_1 \ldots \mathrm{d}\tau_N. \quad (25)$$

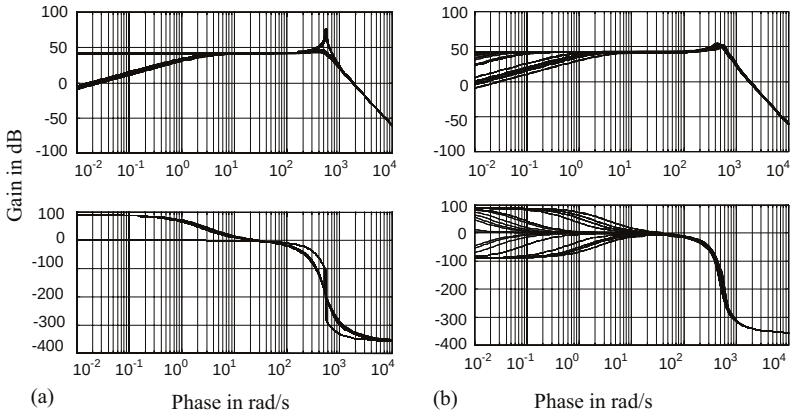

Fig. 3. Degree-1 term of the Volterra series of: (a) nonlinear plant; (b) input–output linearized plant, for the nominal and the perturbed states.

The response of this system to the input signal

$$u(t) = \sum_{p=1}^{P} e^{j\omega_p t} \tag{26}$$

is defined by

$$Y(t) = \sum_{n=1}^{N} \sum_{p_1,\ldots,p_n}^{P} H_n(j\omega_{p_1}, \ldots, j\omega_{pn}) \prod_{i=1}^{n} e^{(j\omega_{p_i} t)}, \tag{27}$$

which is equivalent to

$$Y(t) = \sum_{n=1}^{N} \sum_{\substack{\text{all combinations} \\ \text{of } P \text{ frequencies} \\ \text{by } n \text{ groups}}} \sum_{\substack{\text{all permutations} \\ \text{of } \omega_{p1},\ldots,\omega_{pn}}} H_n(j\omega_{p_1}, \ldots, j\omega_{pn}) \times \prod_{i=1}^{n} e^{(j\omega_{p_i} t)}. \tag{28}$$

If $P = n$, the function

$$\sum_{\substack{\text{all permutations} \\ \text{of } \omega_{p1},\ldots,\omega_{pn}}} H_n(j\omega_{p_1}, \ldots, j\omega_{pn}) \prod_{i=1}^{n} e^{(j\omega_{pi} t)} \tag{29}$$

is the degree-n symmetric Fourier transform of kernel h_N multiplied by $\prod_{i=1}^{n} e^{(j\omega_{pi} t)}$.

Thus, the Fourier transform of a degree-n symmetric kernel is given by

$$H_n^{\text{sym}} = \frac{1}{n!} \sum_{\substack{\text{all permutations} \\ \text{of } \omega_{p1},..,\omega_{pn}}} H_n(j\omega_{p_1}, \ldots, j\omega_{pn}). \tag{30}$$

Thanks to this growing exponential approach, the Fourier transform of the degree-n term of system (25) is determined, in a practical way, by replacing the input signal $u(t)$ by relation (26) and $Y(t)$ by the expression:

$$Y(t) = \sum_{i=1}^{n} \sum_{\substack{\text{all combinations} \\ \text{of } n \text{ frequencies}}} n! H_n^{\text{sym}}(j\omega_{p_1}, \ldots, j\omega_{p_n}) \prod_{i=1}^{n} e^{(j\omega_{p_i} t)} \tag{31}$$

and then by regrouping the coefficients of the terms $\prod_{i=1}^{n} e^{(j\omega_{pi} t)}$.

4.3. Comparison of the perturbed initial nonlinear plant and the perturbed input–output linearized plant

Using the growing exponential approach the initial nonlinear plant and the input–output linearized plant are represented by Volterra series in the frequency domain. The degree-1 term of the series, which is also the first order linear model, and the degree-2 term can both be represented graphically, but not degree-3 and over.

Fig. 3 compares the frequency responses of the degree-1 term computed from the initial nonlinear plant and from the input–output linearized plant, for the nominal and the perturbed plants. The input–output linearized plant provides better results than the initial nonlinear plant, as parameter variations introduce less uncertainty at high frequencies. At low frequencies, uncertainties being divided by the open-loop gain, their increase following the input–output linearization is not a problem. This result is also visible in the Nichols chart (Fig. 4). Indeed, the frequency uncertainty domains are smaller for the input–output linearized plant than for the nonlinear plant, especially at high frequencies.

Figs. 5 and 6 compare the frequency responses of the degree-2 term computed from the initial nonlinear plant and from the input–output linearized plant, for two different values of the structure. For the input–output linearized plant, the modulus of the degree-2 term is smaller at low frequencies than for the input–output linearized plant and decreases more at high frequencies. This phenomenon is of course accentuated when the actual values of the structure parameters approach the nominal values used for the linearization.

The use of the Volterra representation is not a proof but an indication that the input–output linearization is

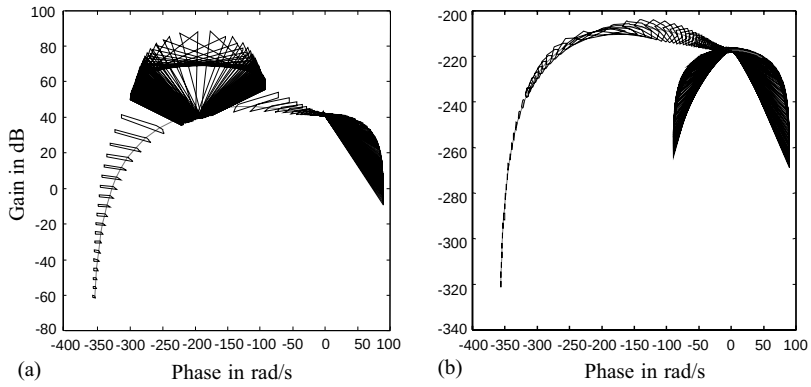

Fig. 4. Nichols locus and uncertainty domains of: (a) initial nonlinear plant; (b) input–output linearized plant.

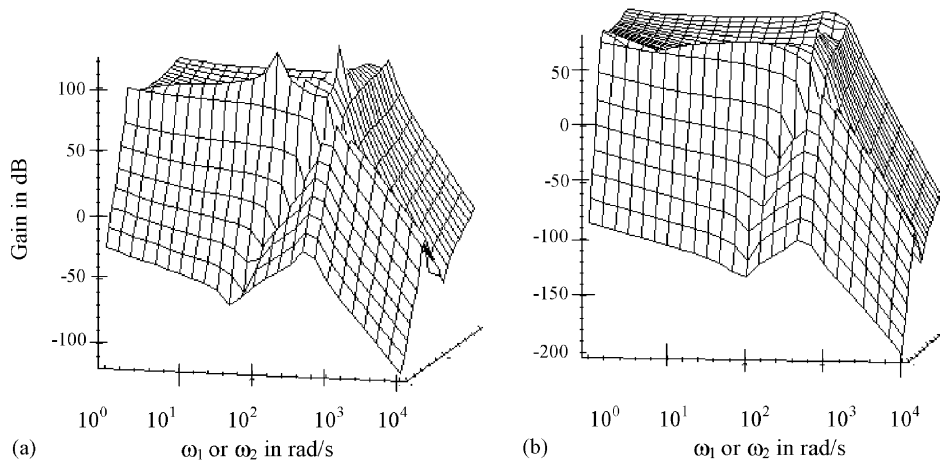

Fig. 5. Degree-2 term of the Volterra series of: (a) nonlinear plant; (b) input–output linearized plant, for the structure defined by: $M = 15\,\mathrm{kg}$, $b = 150\,\mathrm{N/m\,s}$, $c = 75000\,\mathrm{N/m}$.

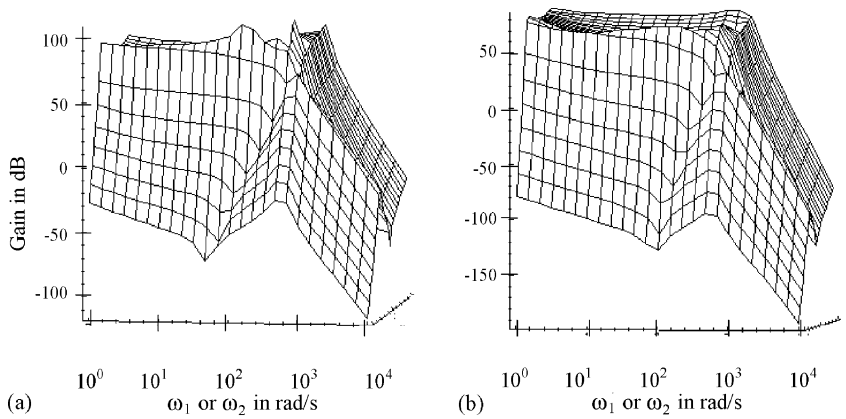

Fig. 6. Degree-2 term of the Volterra series of: (a) nonlinear plant; (b) input–output linearized plant, for the structure defined by: $M = 10\,\mathrm{kg}$, $b = 100\,\mathrm{N/m\,s}$, $c = 50000\,\mathrm{N/m}$.

efficient to reduce the nonlinear character of the initial plant. Hence, the input–output linearized plant is used to design the robust controller of the control-system structure given in Fig. 8. CRONE control-system design is then applied to the set of first order linear models computed from the perturbed input–output "linearized" model (see Section 3.4 and Fig. 3b).

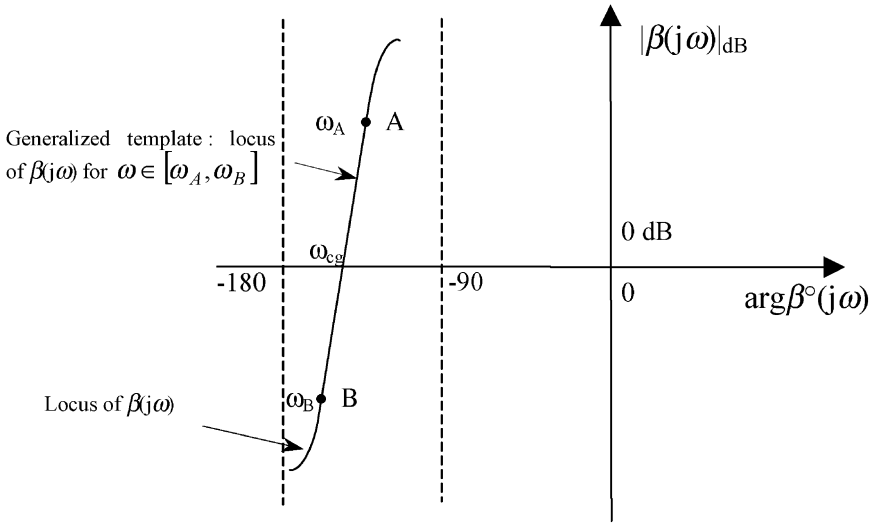

Fig. 7. Representation in the Nichols chart of the generalized template by an any-direction straight line segment.

5. Robust controller design

5.1. CRONE control design method

CRONE control-system design, based on fractional non-integer differentiation (Oustaloup, Lanusse, & Mathieu, 1995, Oustaloup, Sabatier, & Lanusse, 1999), is a frequency approach for the robust control of perturbed plants using the common unity feedback configuration. It consists on determining, for the nominal state of the plant, the open-loop transfer function which guarantees the required specifications (precision, overshoot, rapidity,…). While taking into account the plant right half-plane zeros and poles, the controller is then obtained from the ratio of the open-loop transfer function to the nominal plant transfer function. Three CRONE control generations have been developed, successively extending the application fields (Oustaloup & Mathieu, 1999; Åström, 1999). In this paper, only the principle of the third generation is given. The interests of CRONE control design are multiple. The use of fractional non-integer differentiation permits to define the open-loop transfer function with few high-level parameters. The optimization problem which leads to the optimal transfer function to meet the specifications is thus easier to solve. Moreover, CRONE control design takes into account the plant genuine structured uncertainty domains and not the uncertainty domains given by norms like H_∞ designs. As it is thus less conservative, better performance can be obtained (Landau, Rey, Karimi, Voda, & Franco, 1995). CRONE control design has already been applied to unstable or non-minimum-phase plants, plants with bending modes, and discrete-time control problems (Oustaloup, Mathieu, & Lanusse, 1995).

The third generation CRONE method is based on a particular Nichols locus called a *generalized template* and defined by an any-direction straight line segment around gain cross-over frequency ω_{cg} (Fig. 7). This generalized template is based on the real part (with respect to imaginary unit i denoted $\Re_{/i}$) of fractional non-integer integration (Oustaloup, Levron, Nanot, & Mathieu, 2000):

$$\beta(s) = \left[\cosh\left(b\frac{\pi}{2}\right)\right]^{-1} \Re_{/i}\left[\left(\frac{\omega_{cg}}{s}\right)^{n}\right], \tag{32}$$

with $n = a + ib \in \mathbb{C}_i$ and $s = \sigma + j\omega \in \mathbb{C}_j$. In the Nichols chart at frequency ω_{cg}, the real order a determines the phase placement of the template, and then the imaginary order b determines its angle to the vertical.

In the version of third generation CRONE control design used in this article, the open-loop transfer function defined for the nominal state of the plant, $\beta_0(s)$, takes into account the control specifications at low and high frequencies and a set of band-limited generalized templates around resonant frequency ω_r. Thus $\beta_0(s)$ is defined by

$$\begin{aligned}\beta_0(s) = K\left(\frac{\omega_{-N^-}}{s} + 1\right)^{n_l} \prod_{-N^-}^{N^+} \left(\frac{1 + s/\omega_{k+1}}{1 + s/\omega_k}\right)^{a_k} \\ \times \left(\Re_{/i}\left[\left(C_k \frac{1 + s/\omega_{k+1}}{1 + s/\omega_k}\right)^{ib_k}\right]\right)^{-\mathrm{sign}(b_k)} \\ \times \frac{1}{(1 + s/\omega_{N^+ + 1})^{n_h}},\end{aligned} \tag{33}$$

where

$$\begin{aligned}&C_0 = [(1 + \omega_r^2/\omega_0^2)/(1 + \omega_r^2/\omega_1^2)]^{1/2} \text{ and} \\ &C_k = [\omega_{k+1}/\omega_k]^{1/2} \text{ for } k \neq 0.\end{aligned} \tag{34}$$

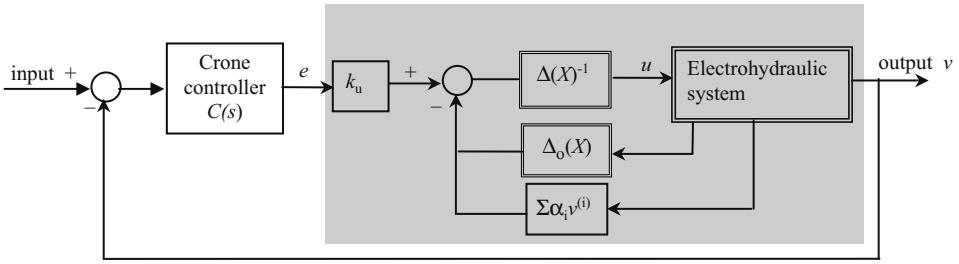

Fig. 8. Control system structure.

K ensures a gain of 0 dB at ω_{cg}, the integer order n_l fixes the steady state behavior of the closed-loop system at low frequencies, and the value of the integer order n_h has to be chosen equal to or greater than the high frequency order of the plant.

CRONE control-system design guarantees the robustness of both stability margins and performance, and particularly the robustness of the maximum M of the complementary sensitivity function magnitude. Let M_r be the required magnitude peak of the complementary sensitivity function for the nominal parametric state of the plant. An indefinite number of open-loop Nichols locus can tangent the M_r Nichols magnitude contour. Also, for perturbed plants, parametric variations lead to variations of M. Thus, an open-loop Nichols locus is defined as optimal if the generalized template around ω_r tangents the M_r Nichols magnitude contour for the nominal state and if it minimizes the variations of M for the other parametric states. By minimizing the cost function $J = (M_{\max} - M_r)^2$ where $M_{\max}$ is the maximal value of magnitude peaks M, the optimal open-loop Nichols locus positions the uncertainty domains correctly, so that they overlap the low stability margin areas as little as possible. The minimization of J is carried out under a set of shaping constraints on the four usual sensitivity functions. Once the optimal open-loop Nichols locus is obtained, the fractional controller $C_f(s)$ is deduced from the ratio of $\beta_0(s)$ to the nominal plant function transfer. The design of the achievable controller consists in replacing $C_f(s)$ by a rational order controller $C_r(s)$ which has the same frequency response.

5.2. Discrete-time design for the electrohydraulic system

Fig. 8 shows the control-system structure with an input–output linearizing feedback (grey tint zone) and a CRONE controller feedback. As the control system is implemented numerically, and as CRONE design is a continuous frequency approach, the discrete-time control-system design problem is transformed into a pseudo-continuous problem using the bilinear w-transformation defined by:

$$z^{-1} = \frac{1-w}{1+w} \text{ with } w = \mathrm{j}v \text{ and } v = \tan\left(\frac{\omega T_s}{2}\right)$$

where T_s is the 1 ms sample period.

So the open-loop transfer function to be optimized is:

$$\beta_0(w) = K\left(\frac{v_{-N^-}}{w} + 1\right)^{n_l} \prod_{-N^-}^{N^+} \left(\frac{1 + w/v_{k+1}}{1 + w/v_k}\right)^{a_k} \times \left(\Re_{/\mathrm{i}}\left[\left(C_k \frac{1 + w/v_{k+1}}{1 + w/v_k}\right)^{\mathrm{i}b_k}\right]\right)^{-\mathrm{sign}(b_k)} \times \frac{f(w)}{(1 + w/v_{N^+ + 1})^{n_h}}, \quad (35)$$

where $f(w)$ is a function that takes into account plant right half-plane zeros which appear when the bilinear w-transformation is applied. For this electrohydraulic system,

$$f(w) = (1-w)\left(1 - \frac{w}{1.26685}\right).$$

Here, optimization uses $N^+ = N^- = 1$, so a set of three band-limited generalized templates is used. The behavior of the open-loop transfer function at low and high frequencies is fixed with: $n_l = 1$ and $n_h = 4$. The required magnitude peak M_r chosen for the nominal plant is 1.2 dB. The constraints on the sensitivity functions are given by:

- the maximum plant input (100 mA),
- the Fourier transform of the required trajectory,
- the maximum magnitude $T_{\max}$ of the complementary sensitivity function set at 3 dB,
- the maximum magnitude $S_{\max}$ of the sensitivity function set at 6 dB.

5.3. Simulation results

Fig. 9 shows the optimal open-loop Nichols locus. The optimized parameters are: $v_r = 0.07$, $v_{-1} = 0.002$, $v_0 = 0.03$, $v_1 = 0.05$, $v_2 = 0.38$, $a_{-1} = 1$, $a_1 = 0.5$, $b_{-1} = 0$, $b_1 = 2$; $T_{\max} = 1.54$ dB and $S_{\max} = 5.7$ dB.

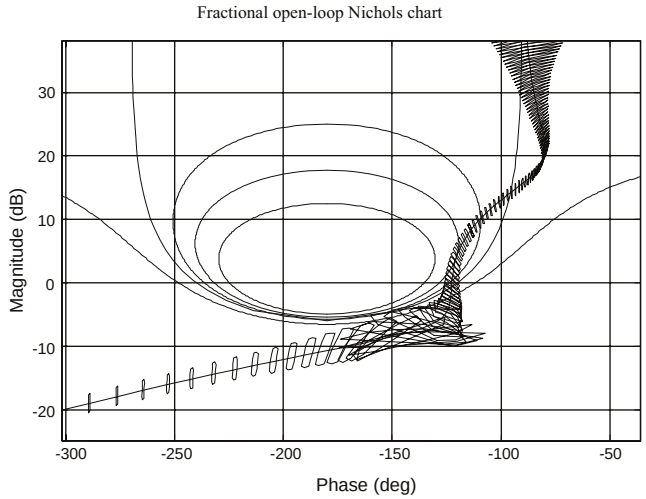

Fig. 9. Optimal open-loop Nichols locus and uncertainty domains.

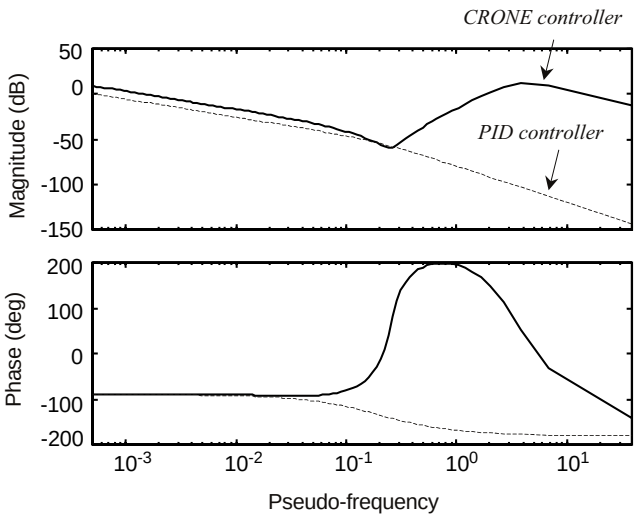

Fig. 10. Bode diagrams of the w-CRONE controller and of the w-PID controller.

The other parameters, computed from the optimized ones, are: $K = 18.5, a_0 = -2$ and $b_0 = -3.8$. The pseudo-continuous rational controller is then defined by

$$C_r(w) = 7.08e^{-4}\left(1+\frac{w}{0.01}\right)\left(1+\frac{w}{0.15}\right) \times \left(1+5.56w+\frac{w^2}{0.0324}\right)\left(1+1.07w+\frac{w^2}{0.0784}\right) \times \left(1+\frac{w}{2.6}\right)w^{-1}\left(1+\frac{w}{0.02}\right)^{-1}\left(1+\frac{w}{0.05}\right)^{-1} \times \left(1+\frac{w}{1.2}\right)^{-1}(1+1.167w+)\left(1+1.11w+\frac{w^2}{3.24}\right) \times \left(1+\frac{w}{18}\right)^{-1}. \quad (36)$$

The discrete-time controller $C(z^{-1})$ is obtained from $C_r(w)$ using the inverse w-transformation defined above.

Results are presented from a simulation of the electrohydraulic system. So that the simulation is nearer to reality as possible, the nonlinear friction force of the hydraulic cylinder is modeled by a 700 N static friction, a 500 N coulomb friction and a Stribeck parameter v_s equal to 0.5 m/s. Moreover, by referring to some sensors data-sheets, noise have been added to the sensor measurements:

- for the acceleration, noise is 0.24 mg and thermal zero offset is 2 mg/°C;
- for the pressure transducers, noise is 60000 Pa and thermal zero offset is 12000 Pa/°C;
- for the displacement transducer, thermal zero offset is 0.075 mm/°C.
- for the velocity transducer, noise is 0.1 mm/s and thermal zero offset is 0.55 mm/s/°C.

Fig. 11a presents the simulated output v obtained with a control-system including the CRONE controller (Fig. 10a) or a common PID controller (Fig. 10b). The PID controller is computed to ensure an open-loop gain crossover pseudo-frequency v_r as big as possible with a gain-margin of 6 dB at least. Its expression is:

$$C_{\mathrm{PID}}(w) = \frac{5\times 10^{-4}}{w(1+w/0.2)}. \quad (37)$$

The CRONE controller gives better results. It permits to have a quicker response by taking into account plant right half-plane zeros and model's uncertainty. Fig. 11b presents the simulated output for three different structures and shows that the cylinder rod can track the trajectory whatever the structure. For the structure with the maximal values, Fig. 12a shows that the servovalve input is less than 100 mA. The input is not totally smooth because of the noise. For other loads, plant inputs are similar. At last, the servovalve displacement y_u is shown on Fig. 12b. y_u is positive as long as the velocity is positive and it happens to be negative during the remaining time. Thus this assumption for the differentiability of the model is not fully verified. But it does not seem to prevent the system from working. The problem of the non-differentiability of the model is a difficult open problem.

6. Conclusion

The robust control of a nonlinear hydraulic plant can be designed using both an input–output linearizing feedback and a linear robust control system. The linear reference model used by the input–output linearizing method must be chosen carefully. The advantage of an input–output linearizing feedback is shown using Volterra representation and using uncertainty domain representation in the Nichols chart. Indeed, this

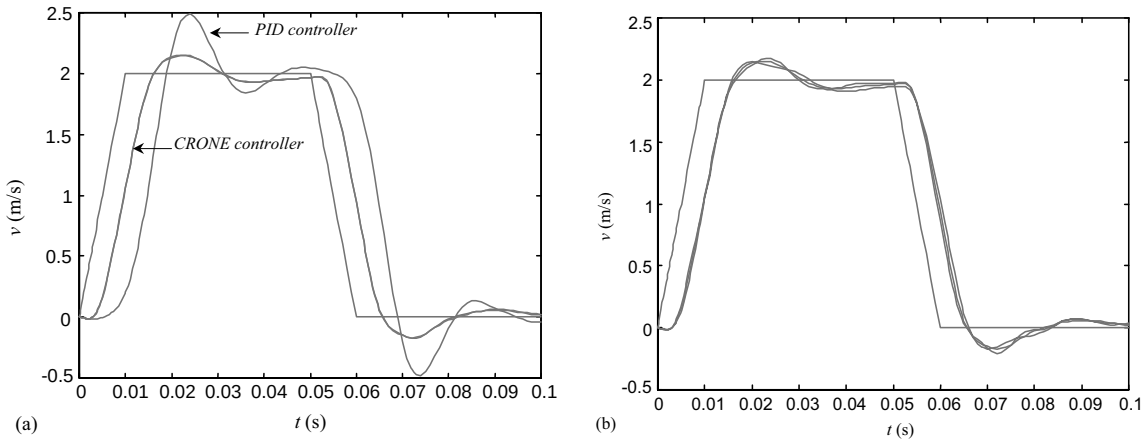

Fig. 11. (a) Simulated output $v(t)$ with the CRONE controller and with a PID controller; (b) Simulated output $v(t)$ with the Crone controller for three different test structures.

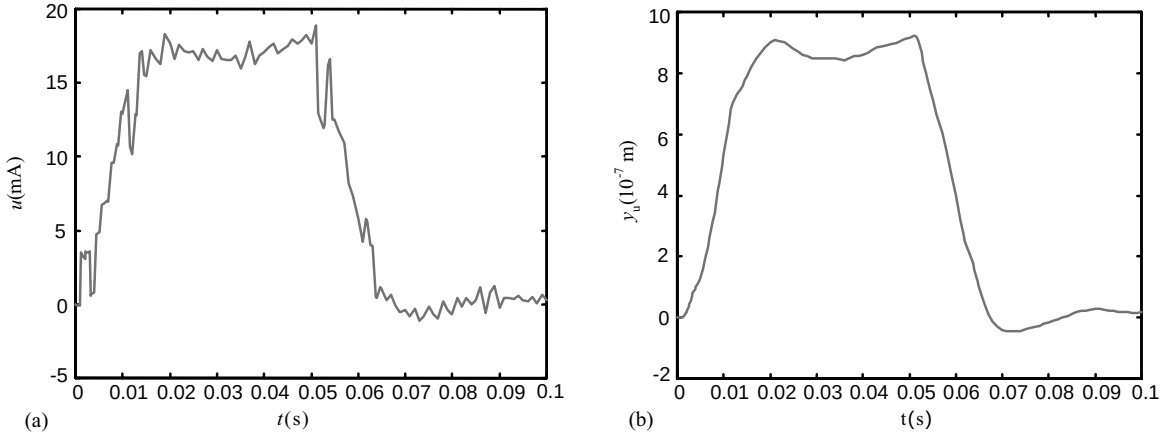

Fig. 12. (a) Servovalve input $u(t)$ for the structure with maximal values; (b) Servovalve displacement.

linearization reduces the effect of the parametric variations of the plant. Moreover, the linearizing feedback can also contain a part of the tracking feedback. Finally, CRONE control design (based on fractional differentiation) is used. It takes into account the uncertainties of the perturbed plant, through a fully structured description which is less pessimistic than most of robust control design approaches. Although a disadvantage of this approach is that it requires state feedback, it is to be noted, that whereas the process considered in the paper is exactly input/output feedback linearizable, the proposed strategy is still efficient when the process is not exactly linearizable. Indeed, the remaining nonlinearities are rejected by the velocity robust feedback.

Final results demonstrate the efficiency of the proposed control-system design method.

References

Åström, K. J. (1999). Model uncertainty and robust control design. *Cosy Workshop—ESF Course*. Valencia, Spain.

Billings, S. A., & Peyton Jones, J. C. (1990). Mapping non-linear integro-differential equations into the frequency domain. *International Journal of Control*, *52*, 863–879.

Brockett, R. W. (1976). Volterra series and geometric control theory. *Automatica*, *12*, 167–176.

Brun, X., Belghardi, M., Sesmat, S., Thomasset, S., & Scavarda, D. (1999). Control of an electropneumatic actuator, comparison between some linear and non linear control laws. *Journal of Systems and Control Engineering, Special Issue ''Controls in Fluid Power System''*, *213*, 387–406.

Cloy, M. C., & Martin, H. K. (1980). *Control of fluid power, analysis and design*. New York: Wiley.

Fossard, A. J., & Normand-Cyrot, D. (1995). *On nonlinear digital control in nonlinear systems*, Vol. 3, Control. London: Chapman & Hall.

Isidori, A. (1995). *Nonlinear control systems* (2nd ed). London: Springer.

Krstic, M., Kanellakopoulos, I., & Kokotovic, P. V. (1995). *Nonlinear and adaptive control design*. New York: Wiley.

Lamnabhi-Lagarrigue, F. (1994). *Analyse des systèmes non linéaires*. Paris: Hermès.

Landau, I. D., Rey, D., Karimi, A., Voda, A., & Franco, A. (1995). A flexible transmission system as a benchmark for robust digital control. *European Journal of Control*, *1*, 77–96.

Levine, W. S. (1996) The control handbook. *CRC Press in collaboration with IEEE press*.

Lesiar, C., & Krener, A. J. (1978). The existence and uniqness of Volterra series for nonlinear systems. *IEEE Transactions on Automatic Control*, *23*, 1090–1095.

Merrit, E. (1967). *Hydraulic control systems*. New York: Wiley.

Olsson, H., Aström, K. J., Canudas de Wit, C., Gäfvert, M., & Lischinsky, P. (1998). Friction models and friction compensation. *European Journal of Control*, *4*, 176–195.

Oustaloup, A., Lanusse, P., & Mathieu, B. (1995). Robust control of SISO plants: The CRONE control. *ECC'95 Conference*. Rome; Italia.

Oustaloup, A., Levron, F., Nanot, F., & Mathieu, B. (2000). Frequency band complex non integer differentiator: Characterization and synthesis. *IEEE Transactions on Circuit and Systems*, *47*, 25–40.

Oustaloup, A., & Mathieu, B. (1999). *La commande crone du scalaire au multivariable*. Paris: Hermès.

Oustaloup, A., Mathieu, B., & Lanusse, P. (1995). The CRONE control of resonant plants: Application to a flexible transmission. *European Journal of Control*, *1*, 113–121.

Oustaloup, A., Sabatier, J., & Lanusse, P. (1999). From fractal robustness to the CRONE Control. *Fractional Calculus and Applied Analysis, An international Journal for Theory and Applications*, *2*, 1–30.

Rugh, W. J. (1981). *The volterra/wiener approach*. Baltimore, Maryland: The Johns Hopkins University Press.

Slotine, J. J. E., & Li, W. (1991). *Applied nonlinear control*. Englewoods Cliffs: Prentice-Hall.